Intermetallics 18 (2010) 1790–1793

Contents lists available at ScienceDirect

Intermetallics

journal homepage: www.elsevier.com/locate/intermet

Short communication

Ni-rich Ni–Pd–P bulk metallic glasses with significantly improved glass-forming ability and mechanical properties by Si addition

Y.Q. Zeng [a], A. Inoue [a,*], N. Nishiyama [b], M.W. Chen [c,*]

[a] Institute for Materials Research, Tohoku University, Sendai 980-8577, Japan
[b] R&D Institute of Metals and Composites for Future Industries (RIMCOF), Sendai 980-8577, Japan
[c] World Premier International (WPI) Research Center, Advanced Institute for Materials Research, Tohoku University, Sendai 980-8577, Japan

ARTICLE INFO

Article history:
Received 14 December 2009
Received in revised form
21 April 2010
Accepted 6 May 2010
Available online 1 July 2010

Keywords:
B. Brittleness and ductility
B. Microalloying
C. Rapid solidification processing

ABSTRACT

We report the significant effect of a small amount of Si on glass formation and mechanical properties of Ni-based bulk metallic glasses. It was found that only 2 at.% silicon dramatically enhances the glass-forming ability of Ni-based Ni–Pd–P alloys and the critical sample diameters can be improved from smaller than 7 mm of $Ni_{60}Pd_{20}P_{20}$ to 15 mm of $Ni_{60}Pd_{20}P_{18}Si_2$. The new Ni-based bulk metallic glass also exhibits excellent mechanical properties with both high strength and good compression plasticity.

1. Introduction

Owing to the unique combination of physical, chemical and mechanical properties and fascinating fabrication capability in supercooled liquid regions, bulk metallic glasses (BMGs) have posed as one of the most promising new materials for structural and functional applications in nanotechnology [1]. Since the late 1980s, numerous bulk glass formers with exceptional glass-forming ability (GFA) have been discovered in various alloy systems [2]. For the case of Ni-based alloys, several bulk glass formers, including Ni–Nb–Cr–Mo–P–B [3], Ni–Nb–Zr–Ti–Co–Cu [4], Ni–Ta–Sn [5], Ni–Zr–Ti–Nb–Si–Sn [6] and Ni–Cu–Ti–Zr–Al–(Si) [7] have been developed in the last ten years. These Ni-based BMGs exhibit superior fracture strength and excellent corrosion resistance. However, they only have very low glass-forming ability with a critical sample diameter (d_c) of 1–5 mm and usually fail in a brittle manner without any compressive plasticity. Recently, on the basis of the traditional $Pd_{40}Ni_{40}P_{20}$ bulk metallic glass [8–11], known as one of the best metallic glass formers since 1970s, we devote to develop economic Ni-rich Ni–Pd–P glasses by reducing the content of expensive Pd [12]. However, the decrease of Pd concentration usually leads to the remarkable loss of GFA [11]. For example, the $Ni_{60}Pd_{20}P_{20}$ alloy only has very limited GFA and cannot be cast into a 7 mm diameter glassy rod even after a careful fluxing treatment [11]. Since minor element additions can obviously improve the GFA of BMGs [13,14], we attempt to look for effective minor elements that can improve the glass-forming ability and mechanical properties of Ni-rich Ni–Pd–P alloys. In this study, we report that a minor Si addition can dramatically enhance the GFA of $Ni_{60}Pd_{20}P_{20}$. A cylindrical $Ni_{60}Pd_{20}P_{18}Si_2$ BMG with a diameter of 15 mm has been successfully produced by using 2 at.% Si replacing P. In addition to the excellent GFA, the new $Ni_{60}Pd_{20}P_{18}Si_2$ BMG also possesses both high fracture strength of above 2 GPa and good compressive plasticity larger than 6%.

2. Material and methods

Mother alloys with nominal compositions of $Ni_{60}Pd_{20}P_{20-x}Si_x$ ($0 \le x \le 10$ at.%) were prepared by melting the mixture of high purity Pd and Ni metals, Si crystal and Ni_3P ingots in evacuated fused silica tubes, and followed by a B_2O_3 fluxing treatment. Ribbon samples with a cross-section of 0.02×1.2 mm^2 were prepared by a single-roller melt spinning technique. Bulk samples were prepared by copper mold casting and water quenching. The amorphous nature of the as-prepared samples was characterized by X-ray diffraction (XRD) with $CuK_{\alpha 1}$ radiation and by transmission electron microscopy (TEM). The thermal properties were studied with a differential scanning calorimeter (DSC) at a heating rate of 0.67 K/s in a purified argon atmosphere. Mechanical properties

* Corresponding authors.
E-mail addresses: ainoue@imr.tohoku.ac.jp (A. Inoue), mwchen@wpi-aimr.tohoku.ac.jp (M.W. Chen).

0966-9795/$ – see front matter © 2010 Elsevier Ltd. All rights reserved.
doi:10.1016/j.intermet.2010.05.003

were examined using an Instron universal material testing system. The gauge dimension of the compression samples is 2 mm in diameter and 4 mm in length. Tested samples were observed with a scanning electron microscope (SEM).

3. Results and discussion

Fig. 1(a) shows the DSC curves of melt-spun $Ni_{60}Pd_{20}P_{20-x}Si_x$ ($x = 0$–10) ribbon samples. Except for $Ni_{60}Pd_{20}P_{10}Si_{10}$, all the ribbon samples exhibit a distinct endothermic glass transition, followed by a supercooled liquid region and then exothermic crystallization. When the concentration of Si is in the range of 0–2 at.%, only one crystallization peak appears in the DSC curves. Further increasing Si contents leads to two separated crystallization peaks. Table 1 summarizes the thermodynamic data of the alloys, including the onset temperature of glass transition (T_g), crystallization (T_x) and melting (T_m), as well as the finishing temperature of melting (T_l). From these experimental data, the quantitative parameters revealing GFA, i.e., ΔT_x ($=T_x - T_g$), T_{rg} ($=T_g/T_l$), and $\gamma = T_x/(T_g + T_l)$, were derived and listed in Table 1. With increasing Si content, T_g increases gradually from 601 K at $x = 0$–639 K at $x = 8$ and disappears at $x = 10$, while T_x first increases from 667 K at $x = 0$–684 K at $x = 2$ and then decreases down to 670 K at $x = 10$. In contrast, both T_m and T_l show a complex changing tendency with increasing Si contents. As a result, ΔT_x, which reflects the resistance to crystallization from the supercooled liquid, first increases by a small amount of Si addition, from 66 K at $x = 0$–74 K at $x = 2$, and then significantly decreases down to 29 K at $x = 8$. The parameters, T_{rg} and γ, which reflect the kinetic stability of undercooled melts, reach their maxima of $T_{rg} = 0.578$ at $x = 3$ and $\gamma = 0.400$ at $x = 4$, respectively. These analyses suggest that the highest GFA of $Ni_{60}Pd_{20}P_{20-x}Si_x$ lies at a composition in the vicinity of $x = 2$–4.

To further determine the best glass former in the $Ni_{60}Pd_{20}P_{20-x}Si_x$ alloy system, the critical sample diameter, d_c, of bulk samples was investigated by copper mold casting. Fig. 2 shows the d_c as a function of Si contents. Cylindrical samples with a single glassy phase can be obtained in the diameter range up to 3.5 mm for $Ni_{60}Pd_{20}P_{18}Si_2$, 2.5 mm for $Ni_{60}Pd_{20}P_{19}Si_3$, and 2.0 for $Ni_{60}Pd_{20}P_{19}Si_1$. All other alloys ($Ni_{60}Pd_{20}P_{20}$, $Ni_{60}Pd_{20}P_{19}Si_4$, $Ni_{60}Pd_{20}P_{14}Si_6$, $Ni_{60}Pd_{20}P_{12}Si_8$, and $Ni_{60}Pd_{20}P_{10}Si_{10}$) cannot be cast into 2 mm diameter glassy rods. Therefore, the $Ni_{60}Pd_{20}P_{18}Si_2$ alloy possesses the highest GFA among $Ni_{60}Pd_{20}P_{20-x}Si_x$ ($x = 0$–10) alloy systems.

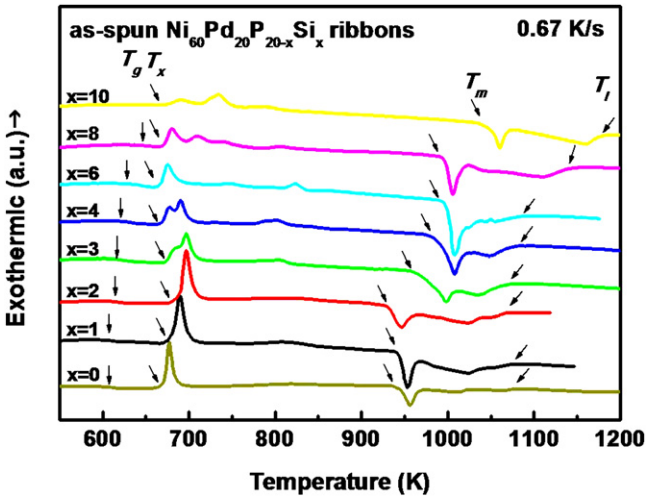

Fig. 1. DSC curves of as-spun $Ni_{60}Pd_{20}P_{20-x}Si_x$ ribbon samples.

Table 1
Thermal analysis data and evaluation parameters for GFA of as-spun $Ni_{60}Pd_{20}P_{20-x}Si_x$ ribbon samples.

Alloys	T_g/K	T_x/K	T_m/K	T_l/K	ΔT_x/K	T_{rg}	γ
$Ni_{60}Pd_{20}P_{20}$	601	667	944	1079	66	0.557	0.397
$Ni_{60}Pd_{20}P_{19}Si_1$	608	673	943	1078	65	0.564	0.399
$Ni_{60}Pd_{20}P_{18}Si_2$	610	684	939	1126	74	0.542	0.394
$Ni_{60}Pd_{20}P_{17}Si_3$	610	673	962	1071	63	0.570	0.400
$Ni_{60}Pd_{20}P_{16}Si_4$	621	670	982	1075	49	0.578	0.395
$Ni_{60}Pd_{20}P_{14}Si_6$	630	671	997	1095	41	0.575	0.389
$Ni_{60}Pd_{20}P_{12}Si_8$	639	668	994	1151	29	0.555	0.373
$Ni_{60}Pd_{20}P_{10}Si_{10}$	–	670	1035	1188	–		–

Moreover, when a repeated B_2O_3 fluxing treatment is employed, cylindrical $Ni_{60}Pd_{20}P_{18}Si_2$ BMG samples with a diameter of 15 mm can be easily cast by water quenching. Fig. 2(b) shows the outer appearance of a ϕ 15 $Ni_{60}Pd_{20}P_{18}Si_2$ sample, which exhibits a lustrous and smooth surface without any concaves or cavities caused by crystallization. The corresponding XRD pattern (Fig. 2(b)) shows only a broad diffraction maximum without any observable crystalline peaks, demonstrating the formation of a fully amorphous structure. TEM characterization further confirms the amorphous nature of the ϕ 15 $Ni_{60}Pd_{20}P_{18}Si_2$ sample and detectable nanocrystallites that may be ignored by XRD have not been found. The DSC curve of the ϕ 15 $Ni_{60}Pd_{20}P_{18}Si_2$ sample in Fig. 2(c) displays the characteristic feature of glassy alloys from glass transition, supercooled liquid region, crystallization to melting with increasing temperature. In comparison with the $Ni_{60}Pd_{20}P_{18}Si_2$ ribbon sample, the ϕ 15 $Ni_{60}Pd_{20}P_{18}Si_2$ sample shows the same glass transition temperature and melting point. However, the bulk sample has a higher crystallization temperature (708 K) and thus larger ΔT_x (97 K) and higher γ (0.408) values, which may be due to the impurity scavenging by the fluxing treatment of the water-quenched bulk samples and the surface effect on the crystal nucleation of the thin ribbons [15–18]. Compared to the $Ni_{60}Pd_{20}P_{20}$ alloy that cannot be fabricated into a ϕ 7 BMG rod after a completely fluxing treatment [11], the formation of the ϕ 15 $Ni_{60}Pd_{20}P_{18}Si_2$ BMG unambiguously demonstrates that the minor Si addition dramatically improves the GFA of the Ni-based Ni–Pd–P alloys.

For the remarkable effect of the Si addition on the GFA of Ni–Pd–P alloys, it may come from two aspects, i.e., strengthened interatomic bonding and suppressed competing crystallization. The glassy $Ni_{60}Pd_{20}P_{18}Si_2$ alloy exhibits a higher T_g (610 K) than that of $Ni_{60}Pd_{20}P_{20}$ ($T_g = 601$ K), indicating the formation of stronger interatomic bonding and denser atomic packing in the $Ni_{60}Pd_{20}P_{18}Si_2$ alloy. However, the fact is that higher Si contents (above 4 at.%) give rise to even higher T_g but the loss of GFA suggests that the enhanced atomic bonding by Si addition is not the main factor for the dramatically improved GFA of $Ni_{60}Pd_{20}P_{18}Si_2$. Considering the 2 at.% Si corresponds to the largest ΔT_x, the suitable Si addition significantly retards the crystallization of supercooled liquid which probably comes from the suppression of heterogeneous crystallization.[11,15,17,18] Since the glass formation is a competing process between the stability of supercooled liquids and crystallization kinetics, the suppression of competitive crystalline phases apparently favors GFA. When the concentration of Si is larger than 2 at.%, two separate crystallization peaks appear in the DSC curves (Fig. 1), indicating high Si content triggers the formation of a primary crystalline phase and leads to the reduction of ΔT_x and γ values.

In addition to the excellent GFA, the $Ni_{60}Pd_{12}P_{18}Si_2$ BMG also exhibits attractive mechanical properties. Different from most Ni-based BMGs that own high strength but low compressive plasticity, the glassy $Ni_{60}Pd_{12}P_{18}Si_2$ exhibits high fracture strength of 2090 MPa and a distinctive plastic strain of 6% (Fig. 3(a)). The fractograph of the $Ni_{60}Pd_{12}P_{18}Si_2$ BMG is shown in Fig. 3(b) from